Available online at www.sciencedirect.com
SCIENCE DIRECT®
Journal of Power Sources 126 (2004) 144–149
JOURNAL OF POWER SOURCES
www.elsevier.com/locate/jpowsour

Synthesis and electrochemical studies on Li–Mn–O compounds prepared at high temperatures

Shuhua Ma*, Hideyuki Noguchi, Masaki Yoshio

Department of Applied Chemistry, Saga University, Saga 840-0852, Japan

Received 19 May 2003; received in revised form 13 August 2003; accepted 25 August 2003

Abstract

The synthesis aspects and electrochemical behaviors of Li–Mn–O compounds prepared at high temperatures of 950–1100 °C were investigated. Heating temperature, oxygen content in reaction atmosphere, and cooling rate affect on the product structure and composition. High heating temperatures favor the expansion of unit cell volume and shrinkage of surface area, and slow cooling rate can diminish only oxygen vacancies and the oxygen absorptions are not enough to affect the lattice parameter and surface area severely. The greatly oxygen-deficient $LiMn_2O_4$ spinels were prepared by following a slow cooling for 10 h to room temperature. In both room and high temperature CV studies, a new oxidation peak at ca. 3.97 V was observed for oxygen-deficient spinel, which was considered coming from an oxidation process related with the 3.2 V discharge plateau. Meanwhile, splits phenomenon of all the two pairs of redox peaks relative to normal $LiMn_2O_4$ spinel was found during high temperature CV measurements at 85 °C. dQ/dV–V plot confirmed the splits. Analysis of the increased capacity at 3.2 V plateau during room and high temperature discharges coupled with surface area revealed that dissolution reaction of Li–Mn–O spinel in electrolyte, which intensified by elevated temperature, caused the growth of oxygen vacancy in spinel structure.

Keywords: Li–Mn–O compounds; Electrochemical behavior; Oxygen vacancy

1. Introduction

Cubic spinel $LiMn_2O_4$ has been being a challenging candidate as cathode material due to its high operating voltage of ca. 4.0 V. An essential factor prevented its application is progressive dissolution in electrolyte upon extended cycling and storage, especially at high temperatures more than 50 °C, which are common for routine uses [1]. Efforts have been devoted to ascertainment of the dissolution mechanism and improvement of cycleability for the material. As insoluble dissolution product, various compounds, e.g., Li_2MnO_3 and $Li_2Mn_4O_9$, etc. have been proposed [2–4]. We have found that CV voltammograms of Li-stoichiometric spinel, $LiMn_2O_4$, suffered a peak split in more than 70 °C for the reduction part of the pair of redox peaks at lower voltage, and attributed it to a process relating to oxygen-deficient spinel [5,6]. Therefore, it is necessary to investigate, comprehensively, the electrochemical behavior of the oxygen-deficient spinel, especially in high temperature.

In this work, the high temperature synthesis for Li–Mn–O compounds were studied by heating at 950–1100 °C and following either rapid or slow cooling process. In rapid cooling, a mixture, composed of main phase of *o*-$LiMnO_2$ and minor phase of $LiMn_2O_4$, was obtained; however, in slow cooling a highly oxygen-deficient Li–Mn–O spinel phase given. The charge/discharge studies at room temperature (RT) and high temperature of 85 °C showed that oxygen vacancies are strongly depended on the cooling conditions, whereas lattice parameter and surface area on the heating temperatures. CV curves and dQ/dV–V plots at 85 °C showed obvious peak splits in positions of both the first and second pairs of redox peaks relative to pristine cubic spinel $LiMn_2O_4$. The work serves as a powerful support for what inferred in the previous paper [6].

2. Experimental

2.1. Preparation

The samples were prepared by heating stoichiometric amount of mixture, molar ratio Li/Mn = 0.5, of γ-MnOOH (Tosoh Co. Ltd.) and $LiOH{\cdot}H_2O$ (Katayama Chemical) at 950–1100 °C in air. The mixture was ground thoroughly

* Corresponding author. Present address: Research & Development Group, Asahi KASEI Corporation, 1-3-1, Yakoh, Kawasaki-Ku, Kawasaki, Kanagawa 210-0863, Japan. Tel.: +81-44-271-3260; fax: +81-44-271-2355.
E-mail address: ma.sb@om.asahi-kasei.co.jp (S. Ma).

0378-7753/$ – see front matter © 2003 Elsevier B.V. All rights reserved.
doi:10.1016/j.jpowsour.2003.08.028

and then preheated at 500 °C for 5 h. After cooling and grinding, it was pressed into a pellet and then calcined again at appointed temperature for 20 h followed by a rapid or slow cooling with different time to room temperature. For rapid cooling, after firing at 1000 °C, the sample was quickly taken out from the furnace and tipped into an agate mortar and then immediately pulverized and ground.

2.2. Structure characterization

The phase identification and the collection of the X-ray diffraction (XRD) data for the structure refinement were carried out using Rigaku RINT1000 X-ray diffractometer (Rigaku Ltd., Japan) with Cu Kα (1.5414 Å) radiation, which was monochromized by a graphite crystal. The XRD data for the structure refinement were collected by a step-scanning mode in the 2θ range of 30–100° with a step width 0.02° and a step time 3 s. Lattice parameter measurement was carried out by the Rietveld method, using the RIETAN profile refinement program [7].

2.3. Electrochemical measurements

Charge/discharge test was carried out in a CR2032 coin-type cell, which consisted of a cathode and a lithium metal anode separated by a Celgard 2400 porous polypropylene film, in which the metallic lithium was in excess. The mixture, which contained 30 mg of accurately weighed electrode material and 10 mg of teflonized acetylene black (TAB-2) as conducting binder, was pressed onto a 16 mm diameter of stainless steel screen disk at 6 t and fabricated into the cell as the cathode after dried at 200 °C for 4 h. The electrolyte used was 1 M $LiPF_6$ ethylene carbonate (EC)/dimethyl carbonate (DMC) 1:2 (v/v). Cells were cycled at a rate of 0.4 mA cm^{-2} (*C*/6).

For cyclic voltammetric measurement, a three-electrode glass cell with a gastight spigot of high compression strength was used. The working electrode was a pellet compacted onto stainless steel gauze, which consisted of 8 mg of tested material and 4 mg of conducting binder TAB-2. The CV measurements were performed with an Arbin Instruments model MSTAT4 battery test system at 0.02 mV s^{-1} scan rate.

The high temperature experiments were carried out in a self-made hot box with oscillation range of ±2 °C. All procedures for handling and fabricating the cells were performed in an argon-filled glove box to avoid possible contamination with water.

3. Results and discussion

3.1. Structure dependence of oxygen-deficient $LiMn_2O_4$ spinel on synthesis conditions

Fig. 1 shows the powder XRD patterns of $LiMn_2O_4$ samples prepared at 950, 1000, 1050 and 1100 °C following slow and rapid cooling processes. All the samples slowly

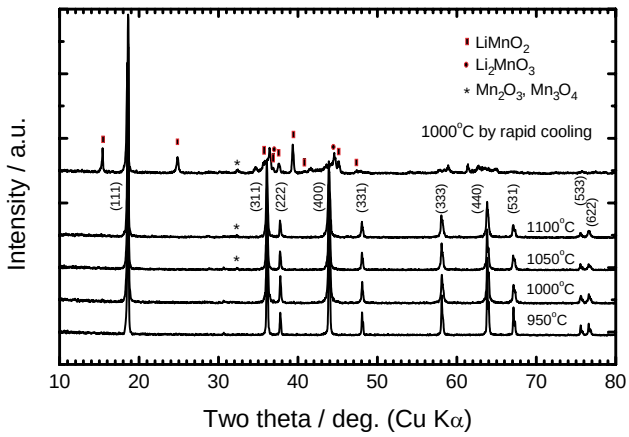

Fig. 1. Powder X-ray diffraction patterns of various $LiMn_2O_4$ spinel samples prepared at high temperatures following slow (950–1100 °C) and rapid (1000 °C) cooling processes.

cooled are pure spinel phase, which could be indexed to $Fd\bar{3}m$ space group with cubic symmetry. A small quantity of impurity phases, Mn_2O_3 and Mn_3O_4, can be detected only for samples treated at high temperatures of 1050 and 1100 °C. When using a rapid cooling, however, complicated reaction products were obtained with main phase of $LiMnO_2$ and the impurity phases of $LiMn_2O_4$, Li_2MnO_3 and Mn_3O_4. Tarascon et al. have studied the structure changes of reaction product with thermal conditions for the preparation of Li–Mn–O spinel [8,9]. Their results displayed that as the increase in quenching temperature, the sample undergoes a series of phase conversions from cubic $LiMn_2O_4$ to a new tetragonal spinel phase and then to decomposition phases of orthorhombic $LiMnO_2$ and Li_2MnO_3. Our work showed a consistent result with them for rapid cooling. However, pure cubic spinel phase was obtained by slow cooling even though heated at high temperatures up to 1100 °C. This result indicates that the phase transformation or decomposition process can be recovered by a slow pseudo-reversible oxygen absorption. By the adjustment of heating temperature, oxygen content in reaction atmosphere, and cooling rate, thus, the preparation of cubic oxygen-deficient spinel samples with various oxygen stoichiometries could be expected. A reaction mechanism can be proposed for these phase transformations based on synthesis conditions as follows [8–13]:

$$LiMn_2O_4 \underset{\text{slow colling}}{\overset{\text{heating at HT}}{\rightleftarrows}} LiMn_2O_{4-z}\ \text{(cubic, oxygen-deficient)} + (z/2)O_2 \underset{\text{slow colling}}{\overset{\text{heating at HT}}{\rightleftarrows}} Li_{1-2z'}Mn_{2-z'}O_{4-z-3z'-z''}\ \text{(cubic, Li, O-deficient and/or tetragonal)} + z'Li_2MnO_3 + (z''/2)O_2 \underset{\text{slow colling}}{\overset{\text{heating at HT}}{\rightleftarrows}} LiMnO_2\ \text{(orthorhombic)} + Mn_3O_4$$

Table 1
Lattice constant and surface area of $LiMn_2O_4$ samples prepared at high temperatures following slow cooling to room temperature for different times

Sample		Surface area ($m^2\,g^{-1}$)	Lattice constant (Å)
Heating temperature (°C)	Cooling time to RT (h)		
700[a]	20	5.30	8.2384
950	10	0.83	8.2499(7)[b]
1000	20	0.79	8.2520(0)[b]
1050	10	0.66	8.2526(6)[b]
1100	20	0.56	8.2547(6)[b]

[a] The 700 °C data are also listed for comparison.
[b] The data are from Rietveld analyses.

The unmatched arrows feature the kinetically quasi-reversible slower oxygen absorption.

We have measured the lattice parameter and surface area in order to clarify the effects of heating temperatures on them. Table 1 summarizes the lattice constant and surface area of oxygen-deficient spinel samples prepared at 950–1100 °C by slow cooling to room temperature with different time. As a reference, the data for that prepared at 700 °C is also listed. It can be found that the surface area and lattice constant depend only on the heating temperature and the cooling rate has no decisive effect on them. A large contraction of surface area, e.g., 84.4% in the case of 950 °C, was made relative to the sample prepared at 700 °C, and meanwhile, the lattice constant expanded as the increase in heating temperature. The result can be considered coming from the oxygen loss as the increase in the heating temperature, which would result in a decrease of attractive force between Mn, with lower valence, and O ions, and thus an expansion of cell volume.

3.2. Electrochemical behavior of oxygen-deficient $LiMn_2O_4$ spinel prepared by slow cooling

3.2.1. Charge/discharge aspect at RT

Fig. 2 shows charge/discharge curves of the initial 1.5 cycles at room temperature of $LiMn_2O_4$ samples prepared at 950–1100 °C following slow cooling for different time to RT. The cooling rates for 950 and 1050 °C are ca. 100 °C h^{-1}, and that for 1000 and 1100 °C are 50 °C h^{-1}. It can be found the cycling curves of all the samples feature typical oxygen-deficient spinel, which exist the plateau at ca. 3.2 V during discharge process [1]. With the increase of heating temperature from 950 to 1100 °C, the capacities of 3.2 V plateau for the samples are capacities of 16.5, 12.3, 14.4 and 12.3 mAh g^{-1}, respectively. There are no apparent relation between heating temperature and the capacity of 3.2 V plateau that quantifies the deficiency of oxygen [13]. Oppositely, quickly cooled samples prepared at 950 and 1050 °C showed higher 3.2 V plateau capacities of 16.5 and 14.4 mAh g^{-1} than the slowly cooled, 12.3 mAh g^{-1}. The result indicates that cooling rate has a decisive effect on the oxygen vacancies. We have concluded that high heating

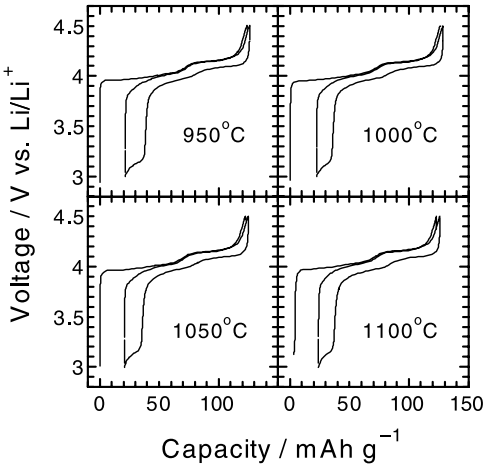

Fig. 2. Charge/discharge curves at room temperature of $LiMn_2O_4$ prepared at 950–1100 °C following slow cooling. Current density: 0.4 mA cm^{-2}; voltage range: 3.0–4.5 V.

temperatures favor the expansion of unit cell volume and shrinkage of surface area by the loss of oxygen as shown in Table 1. It is obvious that the extraction/absorption of oxygen is not a real kinetically reversible process, which features a slower oxygen recovery. The slow cooling, in this case, for 10 or 20 h to RT, can diminish only oxygen vacancies and the oxygen absorptions are not enough to affect the lattice parameter and surface area severely.

3.2.2. Charge/discharge aspect at 85 °C

Some groups have reported that the 3.2 V discharge plateau and 4.5 V charge/discharge plateaus, which are related to oxygen vacancies and lithium deficits, respectively, always exist simultaneously [14–17]. When 4.5 V was used as upper limit of the charging, in this case, no obvious 4.5 V charge/discharge plateaus occurred. This result is consistent with the lithium stoichiometry of the samples, in which Li/Mn = 0.5 was used. However, when the cell was cycled at 85 °C (Fig. 3), obvious 4.5 V charge/discharge plateaus

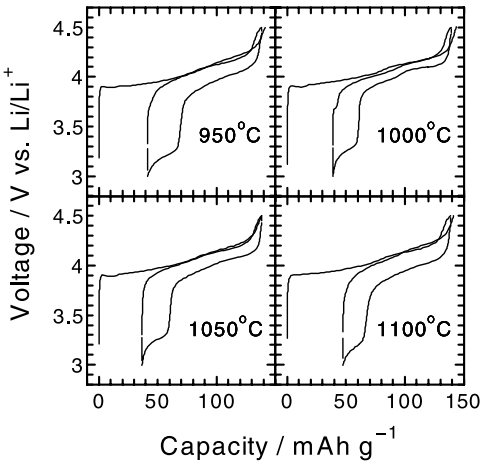

Fig. 3. Charge/discharge curves at 85 °C of $LiMn_2O_4$ prepared at 950–1100 °C following slow cooling. Current density: 0.4 mA cm^{-2}; voltage range: 3.0–4.5 V.

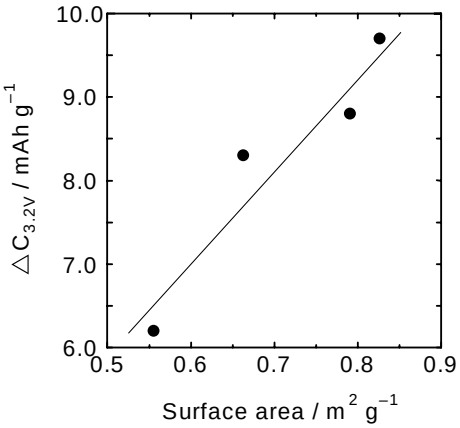

Fig. 4. Plot of the capacity increased in 3.2 V plateau, when cycled at room temperature and 85 °C, vs. surface area of the sample.

occurred and further an enlarged 3.2 V plateau was found relatively to the case at room temperature. They gave values of 26.2, 21.1, 22.7 and 18.8 mAh g^{-1} with the increase of heating temperature from 950 to 1100 °C, respectively. The result demonstrates that more oxygen vacancies and lithium deficits have been produced as the cell was cycled in the high temperature of 85 °C. The increased capacities in 3.2 V plateau, $\Delta C_{3.2\,V}$, are plotted against the surface areas of the samples in Fig. 4. A monotonous change of $\Delta C_{3.2\,V}$ can be found as the increase in specific surface area. The result indicates that the dissolution reaction of the spinel compound intensified by high cycling temperature would be responsible for the above increase of oxygen vacancies.

3.2.3. Cyclic voltammetric measurement

3.2.3.1. CV response at RT. It has been pointed out that the oxygen vacancy of cubic Li–Mn–O spinel can be maximized by the adjustment of heating temperature, oxygen content in reaction atmosphere, and cooling rate. Here, we have prepared the exceedingly oxygen-deficient spinel samples by heating at high temperatures of 950–1100 °C in air following a slow cooling during short periods of 10 or 20 h. For example, the sample prepared at 950 °C following a slow cooling of 10 h gave a 16.5 mAh g^{-1} of capacity for the 3.2 V plateau, which account for 15.7% of the whole discharge capacity. The result shows that there exists a large quantity of oxygen vacancies in the spinel structure. In order to further understand the electrochemical properties of oxygen-deficient spinel samples, we have carried out CV measurements at RT and 85 °C. The results are shown in Fig. 5. It can be found that, at RT, there occurred a new additional peak at ca. 3.97 V, which was overlapped with the normal 4.02 V peak, in the oxidation branch of the first pair of redox peaks. On the other hand, in the reduction branch, no corresponding reduction split peak can be observed around 4 V. In view of the lower peak potential of 3.97 V than the normal reduction peak of 3.99 V, the new peak cannot be attributed to a split of original first oxidation

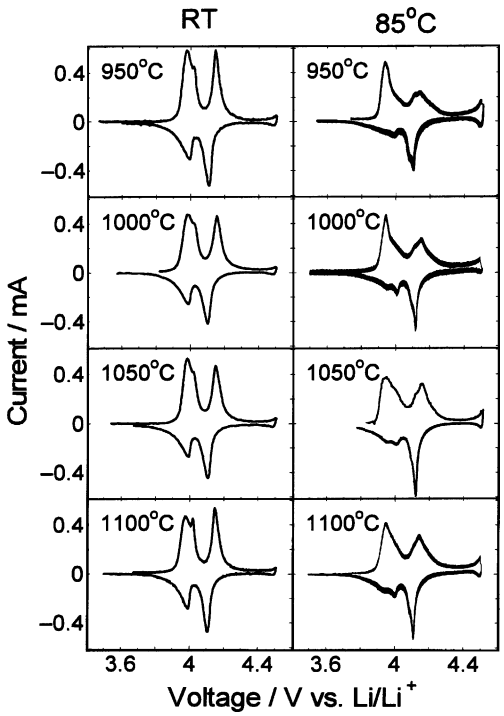

Fig. 5. First cycle of cyclic voltammograms at room temperature and 85 °C for $LiMn_2O_4$ samples prepared at 950–1100 °C following slow cooling. Electrolyte: 1 M $LiPF_6$ EC/DMC (1:2, v/v); scan rate: 0.02 mV s^{-1}, scan range: 3.5–4.5 V vs. Li/Li^+.

peak. We have analyzed the change of peak current of the new peak (3.97 V) between the four samples with different oxygen stoichiometries. The result is plotted in Fig. 6 against the capacity in 3.2 V plateau that was determined by galvanostatic method during cycling at RT. A linear increase in the new peak intensity can be found as the oxygen vacancies were strengthened. The result indicates that the new peak at 3.97 V is caused by the oxygen vacancies in spinel structure. Thus, here, we attribute the new peak to the oxidation branch of the reduction process at ca. 3.2 V.

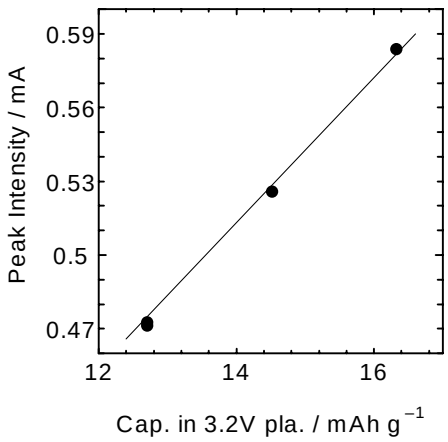

Fig. 6. Plot of peak intensity of the new peak at 3.97 V vs. capacity in 3.2 V plateau during CV scanning and cell cycling at RT for the samples prepared at 950–1100 °C following slow cooling of 10 or 20 h to RT.

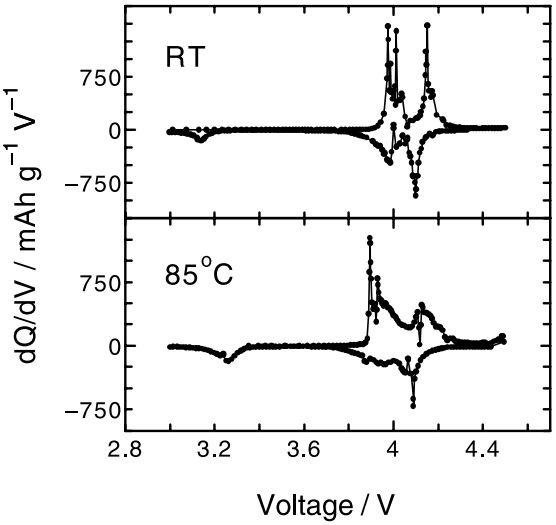

Fig. 7. Differential capacity–voltage relationship from the first charge/discharge curve at RT and 85 °C of $LiMn_2O_4$ sample prepared at 1050 °C following a slow cooling of 10 h to RT.

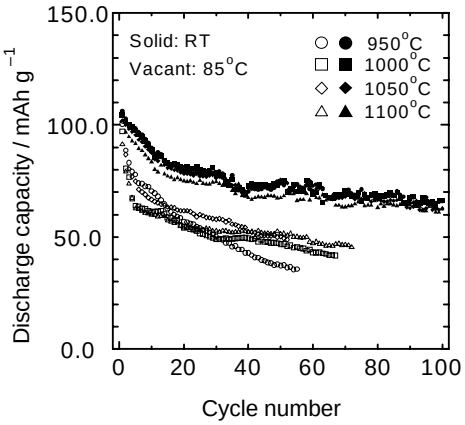

Fig. 8. Changes of discharge capacity with cycle number at room temperature and 85 °C for $LiMn_2O_4$ samples prepared at 950–1100 °C. Electrolyte: 1M $LiPF_6$ EC/DMC (1:2, v/v); current density: 0.4 mA cm^{-2}; voltage range: 3.0–4.5 V vs. Li/Li^+.

3.2.3.2. CV response at 85 °C. The high temperature cyclic voltammetric response of the oxygen-deficient spinels was also studied at 85 °C. From Fig. 5, at lower scan rate of 0.02 mV s^{-1}, obvious peak split phenomenon can be identified for all the four oxygen-deficient samples in this temperature environment of 85 °C, although the split in oxidation branch of the first pair of redox peaks became ambiguous because of the stronger oxidation peak related with the 3.2 V plateau. Yang et al. [18] have found that there exist two two-phase coexisting phase transitions that combined three phases for lithium-rich spinel materials during charge/discharge cycling at RT, on the other hand, Liu et al. [19] also one phase transformation. Here, we found that four one-ordered phase transitions would have occurred in high temperature of 85 °C, but no the split phenomena at RT. More clearly, from the d*Q*/d*V*–*V* plot of the charge/discharge curve for the sample prepared at 1050 °C in Fig. 7, in addition to the sharp peak in 3.97 V from the oxidation branch of the 3.2 V reduction process, at least two pairs of peak splits, four pairs of peaks, can be found at 85 °C, but no splits at RT. The result confirmed the above inference from high temperature CV study. The high temperature XRD isolation of the five phases is necessary. It would be left for our next stage work. We have also found the split phenomenon in reduction branch of the first pair of redox peaks for lithium-stoichiometric spinel prepared at 750 °C when scanned in more than 70 °C [5,6]. In that case, the violent dissolution of lithium-stoichiometric spinel material in electrolyte, due to its higher surface area, was considered to be responsible for the split. From this work, we can see, the oxygen-deficient spinel displayed marked split phenomenon in high temperature, which verified that the dissolution product is oxygen-deficient spinel compound. In view of the smaller surface area and smaller difference in splits among these samples, we strongly thought that the split phenomenon is characteristic of oxygen-deficient spinel compound in high temperature environment. Ceder and Van der Ven have discussed the reasons for the phase separation in lithium intercalation host compounds from first principles [20]. Here, we, analogous to staging insertion of Li^+ ions in graphitic carbon, tentatively consider the split is relating to the domain separation of intercalatable vacancies, 8a and 16d sites, energetically caused by more extensive O and Li deficits at high temperature environment.

3.2.4. Cycling performance

Fig. 8 shows the cycling behaviors of the four oxygen-deficient samples at RT and 85 °C. It can be found that at RT, as expected, the samples give higher capacity than at

Table 2
Discharge capacity and fading rate at room temperature and 85 °C for $LiMn_2O_4$ samples prepared at 950–1100 °C following slow cooling

Heating temperature (°C)	Room temperature				85 °C			
	Discharge capacity			Fade rate ($(C_{10} - C_{50})/C_{10}$, %)	Discharge capacity			Fade rate ($(C_{10} - C_{50})/C_{10}$, %)
	1st	10th	50th		1st	10th	50th	
950	106.18	89.69	73.97	17.53	109.89	75.10	46.73	37.78
1000	104.67	88.78	74.35	16.25	104.45	70.95	46.78	34.07
1050	104.10	87.54	75.68	13.55	101.68	66.76	50.14	24.90
1100	101.87	83.48	67.46	19.19	96.88	65.03	51.60	20.65

85 °C. More clearly, from Table 2, at RT, with the increase of heating temperature the discharge capacity decreased, but meanwhile, the cycling performance was improved. In 85 °C, the same result was obtained, except the rapider capacity fading. The improved cycling performance in high heating temperature is considered coming from the smaller surface area, which gives a weaker dissolution of the spinel sample in electrolyte. The result suggests that even for the highly oxygen-deficient spinel compounds, the dissolution also take an important effect on the cell property of the spinel electrode.

4. Conclusions

The synthesis and electrochemical behaviors of Li–Mn–O compounds prepared at high temperatures of 950–1100 °C followed rapid and slow cooling were investigated.

A mixture with main phase of *o*-$LiMnO_2$ was obtained using rapid cooling. On the other hand, pure cubic oxygen-deficient $LiMn_2O_4$ spinels were gotten using slow cooling. Kinetically quasi-reversible slower oxygen absorption was believed to be responsible for the obtained samples. By adjustment of heating temperature and cooling rate, the preparation of cubic oxygen-deficient spinel samples with various oxygen stoichiometries can be achieved. The heating temperatures have decisive effect on surface area and lattice parameter, whereas the cooling rate on oxygen vacancies.

Electrochemical behaviors at room temperature and 85 °C of highly oxygen-deficient Li–Mn–O spinel were studied. A new peak at ca. 3.97 V in the oxidation branch of first pair of redox peaks was observed for oxygen-deficient spinel samples. The peak was considered coming from an oxidation process related with the 3.2 V discharges plateau.

CV studies at elevated temperature showed that oxygen-deficient $LiMn_2O_4$ spinel undergoes a series of phase separations induced by high environment temperature along with the extraction/insertion of Li^+ ions.

High temperature discharge studies revealed the dependence of the increase of oxygen vacancy on surface area. It was concluded that dissolution reaction of Li–Mn–O spinel in electrolyte, which intensified by elevated temperature, causes the aggravation of oxygen vacancy in spinel structure.

Acknowledgements

The authors are grateful to the grants-in-aid for Scientific Research from the Japanese Ministry of Education for financial support of this research.

References

[1] M.M. Thackeray, P.J. Johnson, L.A. De Picciotto, P.G. Bruce, J.B. Goodenough, Mater. Res. Bull. 19 (1984) 179.
[2] A. Blyr, C. Sigala, G. Amatucci, D. Guyomard, Y. Chabre, J.M. Tarascon, J. Electrochem. Soc. 145 (1998) 194.
[3] S.J. Wen, T.J. Richardson, L. Ma, K.A. Striebel, P.N. Ross Jr., E.J. Cairns, J. Electrochem. Soc. 143 (1996) L136.
[4] A.D. Robertson, S.H. Lu, W.F. Howard Jr., J. Electrochem. Soc. 144 (1997) 3505.
[5] S. Ma, H. Noguchi, M. Yoshio, in: Proceedings of Sixth International Meeting on Lithium Batteries, No. 194, Como, Italy, May 2000.
[6] S. Ma, H. Noguchi, M. Yoshio, J. Power Sources, submitted for publication.
[7] F. Izumi, Nippon Kessho Gakkai Shi 27 (1985) 23.
[8] J.M. Tarascon, E. Wang, F.K. Shokoohi, W.R. McKinnon, S. Colson, J. Electrochem. Soc. 138 (1991) 2859.
[9] J.M. Tarascon, W.R. McKinnon, F. Coowar, T.N. Bowmer, G. Amatucci, D. Guyomard, J. Electrochem. Soc. 141 (1994) 1421.
[10] A. Yamada, K. Miura, K. Hinokuma, M. Tanaka, J. Electrochem. Soc. 142 (1995) 2149.
[11] M.M. Thackeray, M.F. Mansueto, D.W. Dees, D.R. Vissers, Mater. Res. Bull. 31 (1996) 133.
[12] M.M. Thackeray, M.F. Mansueto, J.B. Bates, J. Power Sources 68 (1997) 153.
[13] Y. Yagi, Y. Hideshima, M. Sugita, H. Noguchi, M. Yoshio, Electrochemistry 68 (2000) 252.
[14] M.R. Palacin, Y. Chabre, L. Dupont, M. Hervieu, P. Strobel, G. Rousse, C. Masquelier, M. Anne, G.G. Amatucci, J.M. Tarascon, J. Electrochem. Soc. 147 (2000) 845.
[15] Y. Gao, J.R. Dahn, J. Electrochem. Soc. 143 (1996) 100.
[16] Y. Gao, J.R. Dahn, Solid State Ionics 84 (1996) 33.
[17] G.G. Amatucci, C.N. Schmutz, A. Blyr, C. Sigala, A.S. Gozdz, D. Larcher, J.M. Tarascon, J. Power Sources 69 (1997) 11.
[18] X.Q. Yang, X. Sun, S.J. Lee, J. McBreen, S. Mukerjee, M.L. Daroux, X.K. Xing, Electrochem. Solid State Lett. 2 (1999) 157.
[19] W. Liu, K. Kowal, G.C. Farrington, J. Electrochem. Soc. 145 (1998) 459.
[20] G. Ceder, A. Van der Ven, Electrochim. Acta 45 (1999) 131.